

Laser direct patterning of a reduced-graphene oxide transparent circuit on a graphene oxide thin film

Cite as: J. Appl. Phys. **113**, 244903 (2013); <https://doi.org/10.1063/1.4812233>

Submitted: 03 May 2013 . Accepted: 07 June 2013 . Published Online: 26 June 2013

K. C. Yung, H. Liem, H. S. Choy, Z. C. Chen, K. H. Cheng, and Z. X. Cai



View Online



Export Citation



CrossMark

ARTICLES YOU MAY BE INTERESTED IN

[Post-fabrication, in situ laser reduction of graphene oxide devices](#)

Applied Physics Letters **102**, 093115 (2013); <https://doi.org/10.1063/1.4794901>

[Direct laser-enabled graphene oxide-Reduced graphene oxide layered structures with micropatterning](#)

Journal of Applied Physics **112**, 064309 (2012); <https://doi.org/10.1063/1.4752752>

[Fast growth of graphene patterns by laser direct writing](#)

Applied Physics Letters **98**, 123109 (2011); <https://doi.org/10.1063/1.3569720>

Lock-in Amplifiers
Find out more today



Zurich
Instruments

Laser direct patterning of a reduced-graphene oxide transparent circuit on a graphene oxide thin film

K. C. Yung,^{a)} H. Liem, H. S. Choy, Z. C. Chen, K. H. Cheng, and Z. X. Cai
 Department of Industrial and Systems Engineering, The Hong Kong Polytechnic University, Hung Hom, Kowloon, Hong Kong

(Received 3 May 2013; accepted 7 June 2013; published online 26 June 2013)

In this study, reduced-graphene oxide (GO) circuits were directly patterned on glass using an industrially available excimer laser system. A threshold of laser energy density was observed, which provided a clear differentiation on whether the GO was reduced. A sharp drop of resistance by a factor of 10^4 was measured as the laser energy density increased from 65 to 75 mJ/cm². The highest conductivity measured was $\sim 1.33 \times 10^4$ S/m, which is among the best reported in the literature for any laser reduction method. Raman analysis of the excimer laser-reduced GO film revealed the formation of a prominent *2D* peak at 2700 cm⁻¹. The relative signal strength between the Raman *D* and *G* peaks suggests that the amount of structural disorder in the reduced GO is insignificant. The reduced GO displays a transmittance greater than 80% across the entire range from 450 to 800 nm. The outstanding electrical, optical, and morphological properties have enabled graphene to display promising applications, and this nano-processing method makes graphene even more attractive when used as a transparent electrode for touch screens and in many more applications. © 2013 AIP Publishing LLC. [<http://dx.doi.org/10.1063/1.4812233>]

INTRODUCTION

Graphene is a flat monolayer of *sp*²-hybridized carbon atoms tightly packed into a two-dimensional (2D) honeycomb structure. It has attracted growing attention owing to its superior thermal conductivity, electrical conductivities, and mechanical strength that rivals the notable in-plane values of graphite (~ 3000 W/m K, 8000 S/m, and 1000 GPa, respectively).^{1,2} Much research has focused on its fabrication since its first creation by micro-exfoliation in 2004.³ Besides micro-exfoliation, fabricating methods developed include thermal chemical vapor deposition techniques,⁴⁻⁶ plasma enhanced chemical vapor deposition,⁷⁻⁹ chemical methods,¹⁰ thermal decomposition of SiC,¹¹⁻¹³ un-zipping CNTs,^{14,15} etc. In this study, a nano-second laser is used to selectively reduce graphene oxide (GO) to fabricate pre-defined graphene patterns. It has many advantages including fast prototyping, reduced technical steps, high throughput, no chemicals, environmentally friendly, high yields, high resolution, and precision.

Atomic force microscopy (AFM) has been the primary method used to identify single and multi-layers of graphene on substrates.^{3,16} However, this method suffers from low throughput. In addition, due to the low chemical contrast, only one and two layers of graphene films can be identified by AFM if folds or wrinkles are present.^{3,16} Raman spectroscopy is a widely used method for characterizing carbon-containing products, especially considering conjugated and double carbon-carbon bonds exhibit high Raman intensities. Graphene's electronic structure can be uniquely identified in its Raman spectrum.¹⁷ Raman fingerprints for single layers, bi-layers, and multi-layers reflect changes in the electron bands, providing an unambiguous, high-throughput, and non-destructive probe to identify the graphene layer.

The Raman spectrum of graphene has two prominent peaks: the *G* and *2D* peaks, which lie at around 1580 and 2700 cm⁻¹, respectively. The *G* peak is due to the doubly degenerate zone center *E*_{2g} phonon (in-plane optical mode).¹⁸ The *2D* peak is the second order of zone-boundary phonons. These phonons require no defects for their activation.¹⁹ Single-layer graphene has a sharp, single *2D* peak, in contrast to graphite and multi-layered graphene.¹⁹ Zone boundary phonons do not satisfy the Raman fundamental selection rule, as they are not observed in first order Raman spectra of defect-free graphene.²⁰ They give rise to a peak at ~ 1350 cm⁻¹ in defective graphene, named the *D* peak.¹⁸ The *D* peak is caused by the breathing modes of the *sp*₂ atoms and a defect is required for its activation.^{18,21-23} If the structural defects in graphene are not sufficient to activate the *D* peak, it can only be observed at the edges.

Graphene is a zero-bandgap semiconductor with a linear band structure near the *k*-point. At high optical intensities, the photo-generated carriers block further absorption. The high frequency conductivity for Dirac fermions in graphene should be a universal constant equal to $e^2/4\hbar$. This unique property gives graphene a universal 2.3% linear optical absorption that makes it transparent, despite its high conductivity.

Figure 1 shows the general procedure to additively fabricate conducting micro-circuits with graphene which is patterned and reduced from graphene oxide by an excimer laser. Photochemical reactions between GO and laser light is complex. As shown in Figure 1, there are C-C bonds and C-O bonds around the graphene (C=C bond) in graphene oxide. A C=C bond is 13% shorter but 76% stronger than that of a C-C bond, whereas a C=O bond is 15% shorter but over 100% stronger than a C-O bond. It is believed that the photon energy of light will cleave a C-C bond and C-O bond in GO first because the C=C bond is stronger than the C-C

^{a)}Email: wincokc.yung@polyu.edu.hk.

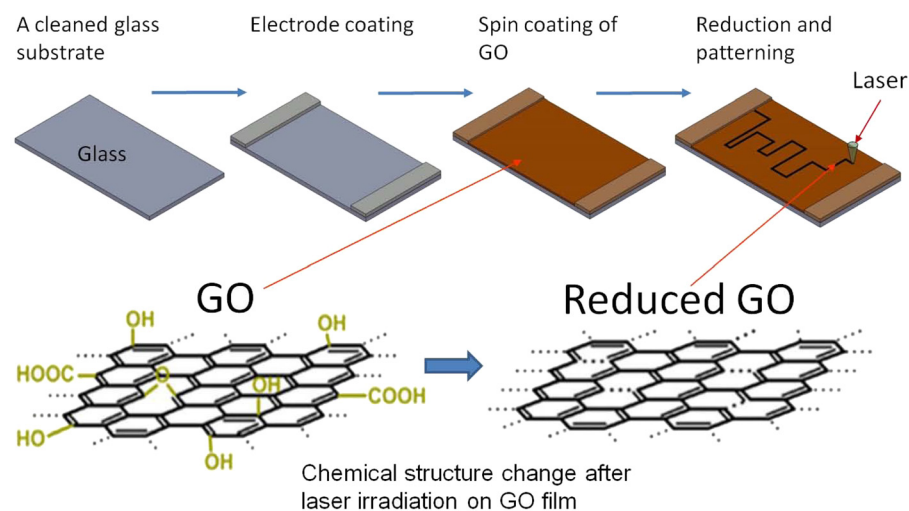


FIG. 1. Schematic of reduction of GO by laser. The black circuit represents reduced GO.

bond and C–O bond. GO is then reduced to graphene. A previously ultrasonic and plasma cleaned soda lime glass for indium tin oxide (ITO) application is dip-coated with GO suspensions in water. The thickness and evenness of the GO film can be modified by changing the dipping volume and temperature of the glass substrate. Laser direct patterning is a mature technology in industry, and versatile micro and nano-circuits can be patterned on GO with the method described above.

In this paper, we employ 248 nm excimer laser light to examine the role of pulsed deep-UV on the reduction of a GO film. Raman spectra, resistance measurement, with various laser energy densities, are present. The results collectively demonstrate that a laser pulse is able to reduce a GO film with good electrical conductivity. The mechanisms and the potential utility of this approach in circuit fabrication strategies are briefly discussed. In addition, the reduced graphene has good optical transparency and is mechanically flexible in nature; graphene-based circuits and electrodes can be used to replace the increasingly expensive ITO in touch-screen displays, photovoltaic solar cells, and LED lighting. The merging of the well-established excimer laser lithographic techniques with the demonstrated approach for GO reduction highlights the possibility of fast, large-scale micro-patterning of graphene features in the near future.

EXPERIMENTAL

Single layer graphene oxide dispersed in water was purchased from Graphene Laboratories, Inc., NY, with a composition of 79% carbon and 20% oxygen and a concentration of 500 mg/l. The flake size was in the range of 0.5–5.0 μm . The GO solution was spun coated at 3000 rpm on the glass, and dried at 95 $^{\circ}\text{C}$ for 30 min. It is worth mentioning that the temperature of the glass substrate should not exceed 100 $^{\circ}\text{C}$, at which temperature GO begins to be reduced. The as-prepared GO film was used for further processing by a nano-second laser.

The laser reduction experiment was performed using a GSI Lumonics PulseMaster PM-848 KrF excimer laser (20 ns pulse width and 200 $\mu\text{m/s}$ scan speed) with a wavelength of 248 nm. A 300 \times 300 μm^2 aperture was imaged

onto the sample at approximately 30:1 reduction using a projection beamline, and produced a rectangular spot on the GO film of size $\sim 10 \times 10 \mu\text{m}^2$. To observe the change in GO film resistance as a function of laser energy, the laser was operated at a repetitive rate of 1 Hz, and its output energy density was controlled in a range from 60 to 190 mJ/cm^2 . To complete the laser reduction, the GO film was pre-treated with one pulse at an energy density of 65–75 mJ/cm^2 , followed by an additional 2–3 shots. The reduced GO was observed under optical microscope. The patterned depth was measured by an optical profiler, Wyko NT9000 optical profiling system with sub-nanometer resolution. Unpolarized Raman spectra on the GO film were obtained using a Renishaw 2000 confocal Raman spectrometer using 514 nm excitation with a $\times 50$ objective. Resistances of reduced-GO circuits were measured with a Fluke 73 series III and insulation resistance measurement system AMI-050-P. UV-Vis absorption spectroscopy characterization was performed on LAMBDA 650 UV/Vis spectrophotometer (PerkinElmer, USA) in 350–800 nm.

RESULTS AND DISCUSSIONS

Figure 2(a) illustrates a typical result of the laser patterning and reduction of GO. Ablated tracks can be distinctly seen from the line scan of the optical profiler (see Figure 2(b)). The thickness of the as-spun GO was about 40 nm, and the width of the ablated tracks was measured to be 10 μm . The distance between neighboring tracking lines was 15 μm . After laser reduction and patterning, the ablated surfaces could be clearly identified from the surface profiler. The ablated depth was 18–25 nm, which was much thicker than a single layer of graphene, due to the fact that multi-layer GO film was formed by spin-coating. However, the laser-irradiated regions (ablated tracks) still displayed properties of the multi-layer graphene, and is discussed in a later section. The mean roughness of the laser-irradiated region (Figure 2(c)) observed by AFM was 0.54 nm, of the order of the thickness of a single graphene layer. This indicates that the laser energy only breaks the G–O bonds and not the G–G bonds. As a result, the structure of G–G is acceptably preserved. However, the rough edges of laser-irradiated tracks

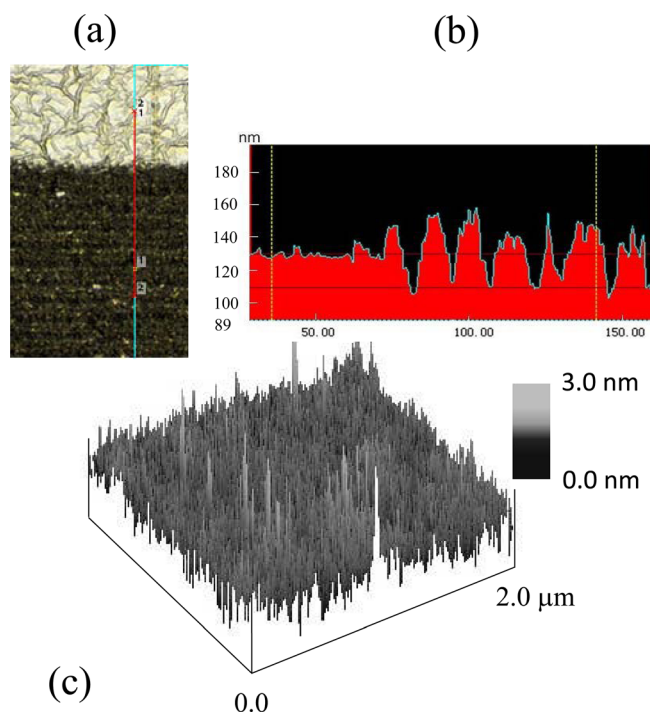


FIG. 2. (a) Optical image of patterned GO lines by laser, (b) step profile of image (a), and (c) AFM 3D topography of the laser-irradiated region.

indicate more severe damage at the edges, which might be due to the steep temperature change taking place at edges so the GO experiences violent photo-thermal effects at the edges.²⁴

Raman spectra of reduced GO

Figure 3(a) represents typical Raman spectra measured for an un-reduced (zero energy density) GO film, and a laser-reduced GO film irradiated at different laser energy densities. The spectra were not normalized. Two main peaks were observed in the spectrum for the un-reduced GO film, *D* (1351 cm^{-1}) and *G* (1590 cm^{-1}). The *G* peak is prominent because of the sp^3 hybridization nature of the GO carbon bonds. Upon excimer laser irradiation with increasing energy density from 60 to 100 mJ/cm^2 , the *D* peak position shifts by 7 cm^{-1} to 1344 cm^{-1} and the intensity is reduced; the *G* peak position shifts by 21 cm^{-1} to 1569 cm^{-1} and a *2D* peak grows at 2700 cm^{-1} , indicating the production of graphitic features. The *D* peak exhibits two features: its position shifts to lower frequencies with increasing incident laser energy density and its relative signal strength (compared to the *G* line) depends essentially on the amount of disorder in the graphene.²³ In our case, the change in relative signal strength is infinitesimal, and it is suggested that the amount of structural disorder in the reduced graphene is insignificant. Further increase in the laser density leads to a prominent *2D* peak (see Figure 3(b)). However, the relative signal strength between the *D* and *G* peaks remains unchanged. The *2D* peaks can be fitted with a single Lorentzian, and the full width at half maximum (FWHM) is $\sim 64\text{ cm}^{-1}$. Previous work suggested that the *2D* peak fitted with a single Lorentzian profile having a typical FWHM between 50 and 65 cm^{-1} could reveal the presence of turbostratic graphite,²⁵

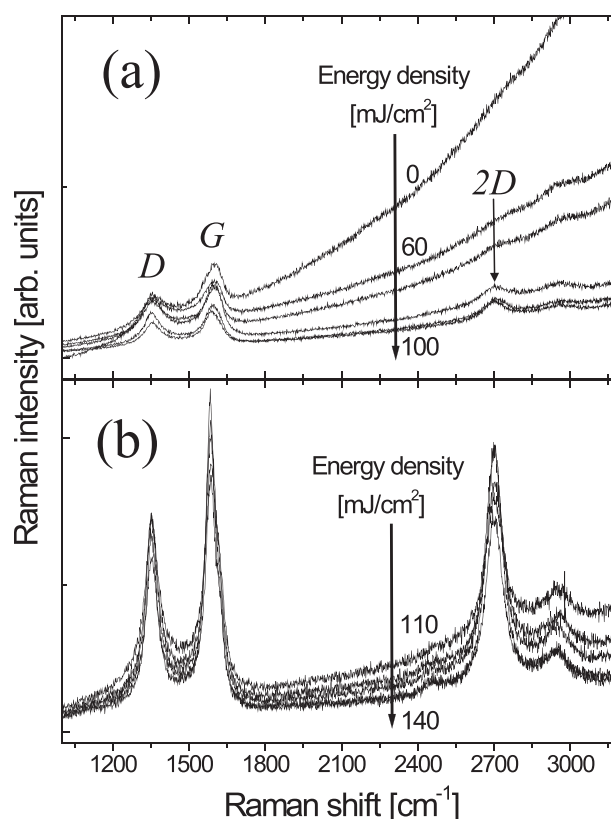


FIG. 3. (a) Unpolarized Raman spectra of un-reduced GO compared with spectra of laser-reduced GO with various energy densities (60-100 mJ/cm^2), and (b) Raman spectra from reduced GO with higher energy densities.

which is composed of multiple randomly oriented graphene sheets.^{26,27} A bi-layer graphene structure exhibits a much broader and up-shifted *2D* band with respect to graphene. This band is also quite different from that of bulk graphite. In Figure 3(b), the presence of the Raman *D* peaks in the laser-reduced GO spectra obtained at higher energy densities can be attributed both to the remaining oxygen species present after the reduction and to the defects associated with the edge scattering in the graphene sheets. Alternatively, the laser reduced top GO layer has underlying GO support, and this can partially contribute to the Raman *D* band.

To estimate the difference between the GO films in term of order parameters before and after laser-reduction, the mean domain sizes (L_a) in graphene is used.^{28,29} The empirical relationship $L_a\text{ (nm)} = 2.4 \times 10^{-10} \lambda_1^4 (I_D/I_G)^{-1}$ is re-examined, where λ_1 is the probe laser wavelength (nm) and I_D and I_G are the Raman area intensities of the *D* and *G* bands, respectively. From Figures 3(a) and 3(b), the L_a values of 18.8 nm and 29.7 nm were calculated for the untreated and the laser reduced GO, respectively. An increase in the L_a value suggests that the laser-reduced graphite oxide evolves to a more ordered state with fewer defects.²⁹

Optical transmittance of reduced GO

Figure 4 shows the optical transmittance from 350 nm to 800 nm for the reduced GO film at different spots within a sample. The transmittance drops rapidly at wavelengths below 400 nm. The reduced GO displays a transmittance greater than 80% across the entire range from 450 to 800 nm.

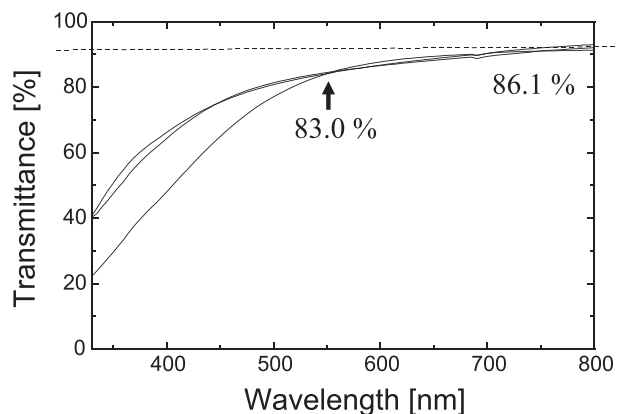


FIG. 4. UV/Vis transmission spectra of reduced-GO film on different spots within a sample. The transmittance is 83% at the most sensitive human eye wavelength 555 nm.

Therefore, the great advantages of the reduced GO circuits are that they have a broad optical transparency, which makes these electrodes highly suitable for transparent electrodes for touch screens, and that they can be made remarkably thin (~ 20 nm) with low surface roughness, and also retain sufficient conductivity.

Resistance of reduced GO

Figure 5 displays the resistance variation of reduced-GO with increasing laser energy densities. A sharp drop of resistance by a factor of 10^4 is measured as the laser energy density increases from 65 to 75 mJ/cm^2 , followed by a gradual decreasing of resistance when the energy density increases from 75 to 110 mJ/cm^2 . The sharp drop indicates that a threshold of laser energy density exists for the reduction of graphene oxide, which is about 70 mJ/cm^2 , after which massive reduction takes place. The reduction of GO is actually a macro-scale bond-breaking of the G-O bond, which occurs only when the laser inducing energy is stronger than the binding energy of the G-O bond. This energy is the threshold of the laser. A considerable decrease in resistance from about 2500 Ω at 75 mJ/cm^2 to 1000 Ω at 100 mJ/cm^2 is followed by a steady increase in resistance to 7900 Ω at 190 mJ/cm^2 . The conductivity was calculated to be $\sim 1.3 \times 10^4$ S/m at 110 mJ/cm^2 . The decrease in resistance is due to the fact that

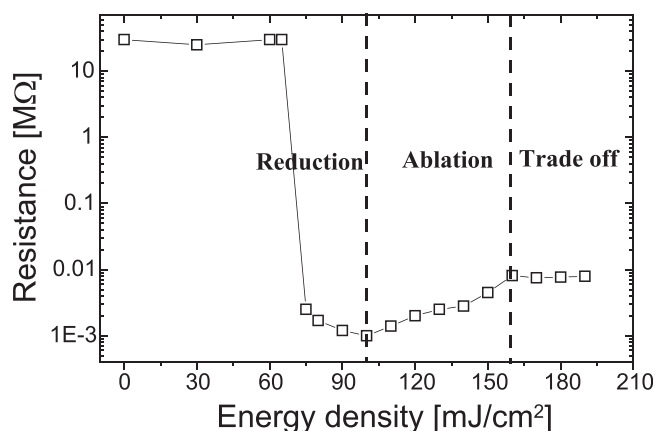


FIG. 5. Resistance of reduced GO as a function of laser energy density. The graph is divided into three regimes with respect to the resistance responding to laser energy density.

more GO is reduced to graphene when the laser energy is increased (the reduction regime is shown in Figure 5). However, the higher laser energy density induces bond-breaking of the G-G bonds, that is, the newly formed not-dense graphene will be ablated by subsequent laser pulsing, leaving the GO exposed to the laser pulse, which induces an abnormal increase in resistance of the laser-irradiated tracks (the ablation regime is shown in Figure 5). Eventually, there will be a trade-off between the newly generated reduced-GO and the ablation of the reduced GO. This induces a plateau in the resistance plot at much higher energy density (the trade-off regime is shown in Figure 5).

CONCLUSIONS

In this work, we have implemented an excimer laser direct reduction technique for patterning nano-metre sized graphene circuits on glass. The laser patterning arises from the oxidative burning of the GO films in air. The nano-second laser directly reduces the patterned graphene nano-circuits. The reduced GO shows significant reduction in resistivity. The quality of the reduced GO was examined by Raman spectroscopy and optical transparency measurement. Specifically, Raman analysis of the excimer laser-reduced GO film revealed the formation of a prominent $2D$ peak at 2700 cm^{-1} . The relative signal strength between Raman D and G peaks remained unchanged, suggesting that the amount of structural disorder in the reduced graphenes is insignificant. The reduced GO has a broad optical transparency. Future work involving improvements of the process by evaluating the effects of substrates and background gases on the laser-GO reduction mechanism is underway and will be reported later.

ACKNOWLEDGMENTS

This work was funded partly by the Hong Kong Polytechnic University under Project no. 4-RPZV and partly by the Hong Kong Innovation Technology Fund (ITF) under Project no. GHP/061/11SZ.

- ¹Y. Zhu, S. Murali, W. Cai, X. Li, J. W. Suk, J. R. Potts *et al.*, *Adv. Mater.* **22**, 3906 (2010).
- ²A. K. Geim and K. S. Novoselov, *Nature Mater.* **6**, 183 (2007).
- ³K. S. Novoselov, A. K. Geim, S. V. Morozov, D. Jiang, Y. Zhang, S. V. Dubonos, I. V. Grigorieva, and A. A. Firsov, *Science* **306**, 666 (2004).
- ⁴P. R. Somani, S. P. Somani, and M. Umeno, *Chem. Phys. Lett.* **430**, 56 (2006).
- ⁵A. N. Obraztsov, E. A. Obraztsova, A. V. Tyurnina, and A. A. Zolotukhin, *Carbon* **45**, 2017 (2007).
- ⁶Q. Yu, J. Lian, S. Siriponglert, H. Li, Y. P. Chen, and S. S. Pei, *Appl. Phys. Lett.* **93**, 113103 (2008).
- ⁷A. N. Obraztsov, A. A. Zolotukhin, A. O. Ustinov, A. P. Volkov, Y. Svirko, and K. Jefimovs, *Diamond Relat. Mater.* **12**, 917 (2003).
- ⁸J. J. Wang, M. Y. Zhu, R. A. Outlaw, X. Zhao, D. M. Manos, and B. C. Holoway, *Appl. Phys. Lett.* **85**, 1265 (2004).
- ⁹J. J. Wang, M. Y. Zhu, R. A. Outlaw, X. Zhao, D. M. Manos, and B. C. Holoway, *Carbon* **42**, 2867 (2004).
- ¹⁰M. Choucair, P. Thordarson, and J. A. Stride, *Nat. Nanotechnol.* **4**, 30 (2009).
- ¹¹C. Berger *et al.*, *J. Phys. Chem. B* **108**, 19912 (2004).
- ¹²E. G. Acheson, U.S. patent 615,648 (1896).
- ¹³D. B. Badami, *Nature* **193**, 569 (1962).
- ¹⁴X. Wang *et al.*, *Angew. Chem.* **47**, 2990 (2008).

- ¹⁵J. Wu, W. Pisula, and K. Mullen, *Chem. Rev.* **107**, 718 (2007).
- ¹⁶K. S. Novoselov *et al.*, *Proc. Natl. Acad. Sci. U.S.A.* **102**, 10451 (2005).
- ¹⁷A. C. Ferrari *et al.*, *Phys. Rev. Lett.* **97**, 187401 (2006).
- ¹⁸H. He, J. Klinowski, M. Forster, and A. Lerf, *Chem. Phys. Lett.* **287**, 53 (1998).
- ¹⁹A. Lerf, H. He, M. Forster, and J. Klinowski, *J. Phys. Chem. B* **102**, 4477 (1998).
- ²⁰M. Hirata, T. Gotou, and M. Ohba, *Carbon* **43**, 503 (2005).
- ²¹T. Szabo, A. Szeri, and I. Dekany, *Carbon* **43**, 87 (2005).
- ²²S. Stankovich, R. D. Piner, S. T. Nguyen, and R. S. Ruoff, *Carbon* **44**, 3342 (2006).
- ²³F. Tuinstra and J. Koenig, *J. Chem. Phys.* **53**, 1126 (1970).
- ²⁴P. Zhao, M. Choudhury, K. Mohanram, and J. Guo, *Nano Res.* **1**, 395 (2008).
- ²⁵D. A. Sokolov, K. R. Shepherd, and T. M. Orlando, *J. Phys. Chem. Lett.* **1**, 2633 (2010).
- ²⁶L. M. Malard, M. A. Pimenta, G. Dresselhaus, and M. S. Dresselhaus, *Phys. Rep.* **473**, 51 (2009).
- ²⁷D. R. Lenski and M. S. Fuhrer, *J. Appl. Phys.* **110**, 013720 (2011).
- ²⁸L. G. Cancado, K. Takai, T. Enoki, M. Endo, Y. A. Kim, H. Mizusaki *et al.*, *Appl. Phys. Lett.* **88**, 163106 (2006).
- ²⁹A. C. Ferrari, *Solid State Commun.* **143**, 47 (2007).